Luminescent properties of Eu^{2+} and Ce^{3+} ions in strontium litho-silicate Li_2SrSiO_4

V.P. Dotsenko [a,*], S.M. Levshov [a], I.V. Berezovskaya [a], G.B. Stryganyuk [b,c], A.S. Voloshinovskii [b], N.P. Efryushina [a]

[a] A.V. Bogatsky Physico-Chemical Institute, Ukrainian Academy of Sciences, Lustdorfskaya doroga 86, 65080 Odessa, Ukraine
[b] Ivan Franko National University of Lviv, Kirilo i Mefodii 8, 79005 Lviv, Ukraine
[c] HASYLAB at DESY, Notkestraße 85, 22607 Hamburg, Germany

ABSTRACT

The luminescent properties of Eu^{2+} and Ce^{3+} ions in Li_2SrSiO_4 have been studied upon excitation in the 2–20 eV region. Based on the results of luminescent measurements, values of the crystal field splitting and the centroid shift of the Ce^{3+} 5d configuration in Li_2SrSiO_4 were found and compared with those of Ce^{3+} ions in some other inorganic compounds. The Eu^{2+} ions in Li_2SrSiO_4 exhibit a broad band emission with a maximum at 576 nm, which is due to the $4f^65d \rightarrow 4f^7$ transition. It was shown that the long-wavelength position of the Eu^{2+} emission in Li_2SrSiO_4 is caused by the large crystal-field splitting of the Eu^{2+} $4f^65d$ configuration and relatively high degree of covalency of the Eu–O bond. The stabilization of Eu^{2+} ions in Li_2SrSiO_4 during the synthesis process requires a strong reducing agent. Two phenomenological approaches to explain the low stability of Eu^{2+} in Li_2SrSiO_4 are also discussed.

© 2010 Elsevier B.V. All rights reserved.

1. Introduction

The white light-emitting diodes (LEDs) are one of the most promising alternatives to conventional electric light sources, i.e. incandesced lamps and Hg-containing fluorescent lamps. This technology implies the use of phosphors for the conversion of the near-ultraviolet (UV) or blue emission from (In, Ga)N LEDs into visible light. For the purpose of efficient conversion, phosphors need to have a number of properties, namely, strong absorption of UV or blue radiation from a LED, high thermal stability and luminescence quenching temperature, good chemical stability, suitable morphology and particle size distribution, low cost [1,2]. For the first time, the concept of white LEDs has been commercially realized by using a combination of a blue LED emitting around 460 nm and yttrium aluminum garnet doped with Ce^{3+} ions ($Y_3Al_5O_{12}:Ce^{3+}$) as a yellow phosphor [3]. This system has several shortcomings, in particularly, a low color rendering index. This stimulates the search for new luminescent materials for LEDs. In recent years, several materials of silicate family, such as $Sr_3SiO_5:Eu^{2+}$ [4], $Sr_3SiO_5:Ce^{3+}$ [5], $Ca_3Si_2O_7:Eu^{2+}$ [6], $M_2MgSi_2O_7:Eu^{2+}$ (M=Ca, Sr, Ba) [6,7], $Sr_2SiO_4:Eu^{2+}$ [8] and $Li_2SrSiO_4:Eu^{2+}$ (Ce^{3+}) [6,9–11], have been presented as promising phosphors for white LEDs. Among these series, materials of

composition $Li_2SrSiO_4:Eu^{2+}$ (Ce^{3+}) gained special attention because of their favorable luminescent properties and a weak thermal quenching of luminescence. Several groups of authors have studied the luminescent properties of Eu^{2+} ions in Li_2SrSiO_4 upon excitation in the 240–550 nm region [6,9–11]. It was found that Eu^{2+}-doped Li_2SrSiO_4 shows a broad band emission with a maximum at about 570 nm. Since this emission is efficiently excited by photons in the 380–460 nm region, quite efficient white LEDs were fabricated by using a combination of (In, Ga)N chips emitting around 420 nm (or 460 nm) and $Li_2SrSiO_4:Eu^{2+}$ as an yellow-orange phosphor [9,10]. Recently, Zhang et al. [11] have found that the emission intensity of Eu^{2+}-doped Li_2SrSiO_4 can be increased by codoping with Ce^{3+} ions. This effect was attributed to an efficient energy transfer from Ce^{3+} to Eu^{2+} ions. Later, Kim et al. [12] have reported that the energy transfer from Ce^{3+} to Eu^{2+} ions does not contribute significantly to the enhanced luminescence of double-doped $Li_2SrSiO_4:Eu^{2+}$, Ce^{3+}. Based on the results of XANES study, these authors came to conclusion that the introduction of Ce^{3+} ions in Li_2SrSiO_4 causes the stabilization of Li-vacancies, and thus suppresses the oxidation of Eu^{2+} ions. Also note that Ce^{3+}-doped Li_2SrSiO_4 has been recently presented as a potential blue phosphor for solid-state lighting [13].

Most studies reported up to now on the luminescent properties of Eu^{2+} and Ce^{3+} ions in Li_2SrSiO_4 are mainly of applied character and a number of basic topics were not even discussed. This paper is focused on the following questions: What factors cause the long-wavelength position of the Eu^{2+} emission in Li_2SrSiO_4? What are the reasons for the low stability of Eu^{2+} ions in Li_2SrSiO_4? To

* Corresponding author.
  E-mail address: ssclab@ukr.net (V.P. Dotsenko).

answer these questions, we have extended the luminescent measurements on Li_2SrSiO_4:Eu^{2+}, Ce^{3+} into the vacuum ultraviolet (VUV) region. One expects that the results presented here can be useful for understanding luminescent properties of other Eu^{2+}-containing oxide phosphors for white LEDs.

It is known that Li_2SrSiO_4 is isostructural with Li_2EuSiO_4 for which Haferkorn and Meyer [14] have given a detailed structure description. Li_2EuSiO_4 belongs to the hexagonal system, with the $P3_121$ space group [14]. In the crystal structure of Li_2EuSiO_4, tetrahedral LiO_4 and SiO_4 are connected by common corners and build up a three-dimensional network that leaves a space for europium (Eu^{2+}) ions which are surrounded by eight oxygen ions. The crystal structure refinement of Li_2SrSiO_4 was performed by Pardha Saradhi and Varadaraju [9] using the Reitveld method and taking Li_2EuSiO_4 as the starting model. These authors found that in Li_2SrSiO_4 each Sr^{2+} ion is coordinated to eight oxygen atoms with Sr–O distances of 2.720 Å ($\times 2$), 2.621 Å ($\times 2$), 2.555 Å ($\times 2$) and 2.536 Å ($\times 2$). It should be also noted that each Si atom is coordinated by four oxygen atoms with Si–O bond distances of 1.722 Å ($\times 2$) and 1.664 Å ($\times 2$).

2. Experimental

Polycrystalline samples of general composition $Li_2Sr_{1-x}Ln_xSiO_4$ (Ln=Eu^{2+}, Ce^{3+}; $x=0.00001-0.007$) were prepared by solid state reaction method. Starting mixtures of Li_2CO_3 (5% excess), SiO_2, $SrCO_3$ and $Ln(NO_3)_3 \cdot nH_2O$ were fired at a temperature of about 600 °C for 6 h in air. The specimens were cooled, mortared to insure homogeneity and fired again at 850 °C for 5 h in air, in a nitrogen stream or in a reducing medium consisting of a nitrogen–hydrogen mixture containing 5% by volume of hydrogen. The samples were checked by X-ray diffraction (XRD) using CuK_α radiation. The results indicate that the final products were formed in homogenous form and their XRD patterns were well matched with JCPDS file no. 47-0120 for Li_2EuSiO_4 and the literature data for Li_2SrSiO_4 [9–11]. No impurity phases were detected in the XRD patterns. The emission and excitation spectra in UV–visible region were recorded at 77 K and room temperature using a Fluorolog Fl-3 (Horiba Jobin Yvon) spectrofluorometer equipped with a xenon lamp. The decay time measurements on Eu^{2+}-doped samples were performed using time correlated single photon counting method upon excitation with a nanosecond LED at 370 nm. The excitation spectra at wavelengths shorter than 330 nm and the luminescence decay kinetics were recorded at 10 K and room temperature using synchrotron radiation and the equipment of the SUPERLUMI experimental station [15] of HASYLAB (Hamburg, Germany). The synchrotron operated in multi-bunch mode with bunches separated by 200 ns. The time-resolved excitation spectra were recorded for several different time intervals after picosecond pulse excitation and corrected for the wavelength dependent excitation intensity with the use of sodium salicylate as a standard.

3. Results

As can be seen from Fig. 1, the emission spectra of $Li_2Sr_{1-x}Eu_xSiO_4$ ($x=0.007$) prepared in air or in inert medium contain several groups of bands in the range 578–710 nm. No doubt that these features are due to the $^5D_0 \rightarrow {}^7F_j$ transitions of Eu^{3+} ions. The excitation spectra for different emission wavelengths appear to be identical. Fig. 2 shows the excitation spectra for the Eu^{3+} emission recorded upon excitation with synchrotron radiation and optical photons. They consist of a broad band with a maximum at about 241 nm and a number of relatively narrow bands at the longer wavelengths. It is evident that the intense band is caused by the
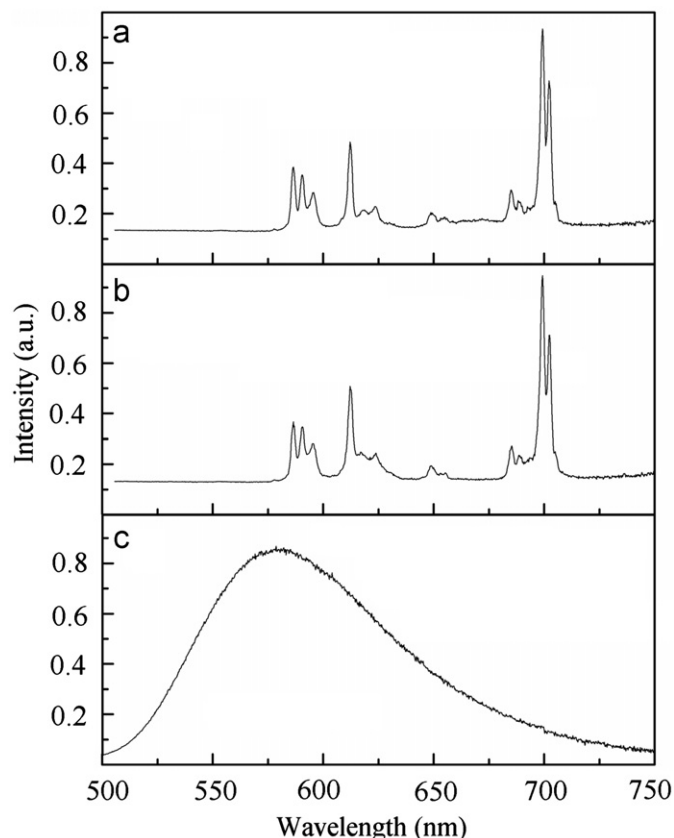

Fig. 1. Emission spectra of $Li_2Sr_{1-x}Eu_xSiO_4$ ($x=0.007$) solid solutions prepared in air (a), in a nitrogen flow (b) and in a reducing medium of 5% H_2/95% N_2 (c). The spectra were recorded at 293 K upon excitation at 395 nm.
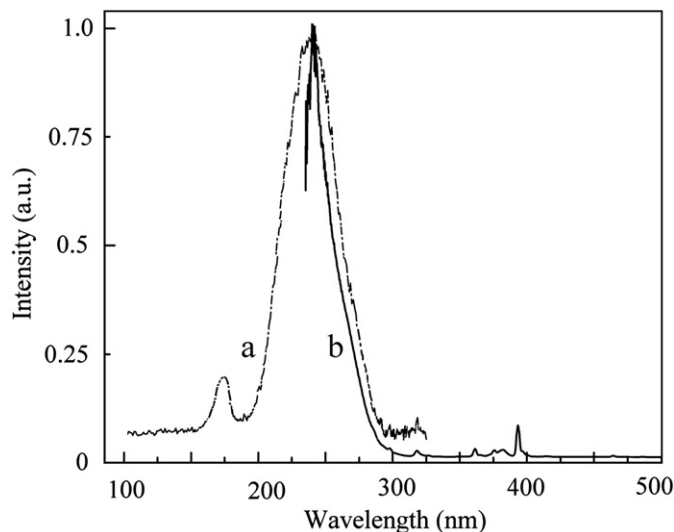

Fig. 2. Excitation spectra of $Li_2Sr_{1-x}Eu_xSiO_4$ ($x=0.007$) for the Eu^{3+} emission ($\lambda_{em}=612$ nm) at 293 K. The spectra were recorded upon excitation with synchrotron radiation (curve a) and optical photons (curve b).

charge transfer (CT) transition from the oxygen 2p states to the empty states of the Eu^{3+} $4f^6$-configuration, while the weaker ones are due to the $4f^6 \rightarrow 4f^6$ transitions of Eu^{3+} ions. The onset of the CT band at 290 nm (4.27 eV) is attributed to the energy threshold of O $2p \rightarrow Eu$ 4f transitions. The (V)UV excitation spectrum (curve a) contains also a band with a maximum at about 175 nm (7.08 eV).

Its origin will be discussed below. Note that the difference between the excitation spectra in the range 230–240 nm is due to the spectral limitations of the UV–visible spectrofluorometer used in this study.

Since both the formal charge and ionic radius of Eu^{3+} differ markedly from those of Li^+, it seems rather unprobable that Eu^{3+} can substitute for Li^+ in any significant amounts. The experimental fact that changing the Eu concentration in the range $x=0.0001–0.007$ has no effect on the emission and excitation spectra confirms the expectation that the Eu^{3+} ions in Li_2SrSiO_4 mainly occupy sites of Sr. Note that the observed position of the Eu^{3+} CT band in Li_2SrSiO_4 ($\lambda_{max}=241$ nm) is close to that for $Sr_2MgSi_2O_7$ ($\lambda_{max}\sim250$ nm) [16], which also contains in its structure eight coordinated Sr-atoms.

No significant changes of the emission spectra of $Li_2Sr_{1-x}Eu_xSiO_4(x=0.007)$ prepared in air or in inert medium were observed upon varying the excitation wavelength in the 240–550 nm region. In other words, no Eu^{2+} luminescence was observed, but only the Eu^{3+} luminescence. As seen from Fig. 1, the Eu^{2+}-related emission band with a maximum at 576 nm is only present in the spectrum of $Li_2Sr_{1-x}Eu_xSiO_4$ ($x=0.007$) prepared in a reducing medium of H_2/N_2. This indicates that the stability of Eu^{2+} ions in Li_2SrSiO_4 is low.

Fig. 3 shows the excitation spectra of $Li_2Sr_{1-x}Eu_xSiO_4$ ($x=0.007$) for the emission at 570 nm at 10 K. The time-integrated spectrum consists of several overlapping bands in the range 230–530 nm. It is evident that these bands are due to excitation of the Eu^{2+} ions via transitions from the $4f^7$ ($^8S_{7/2}$) ground state to the components of the Eu^{2+} $4f^65d$ configuration. The low energy tail of this spectrum exhibits fine structure, which probably reflects the character of the seven (Eu^{3+}) $4f^6$ levels ($^7F_{0-6}$). Also, there is an intense band with an edge at 181 nm (6.85 eV) and a maximum at 174 nm (7.12 eV), which can be tentatively attributed to excitonic absorption. It is difficult to determine the Stokes shift (δ) of the emission at 576 nm, because the lowest-energy excitation band can be too weak to be observed. In view of this, the value of δ was roughly determined from the energy of the zero phonon line, which can be taken as the intersection point of the normalized excitation and emission bands. In Li_2SrSiO_4, the overlap of the excitation and emission spectra occurs at about 525 nm. In this way the Stokes shift of the emission at 576 nm was found to be 3400 cm^{-1}. Upon excitation at 370 nm,

the decay of the emission at 77 and 293 K was found to be single-exponential with a time constant (τ) of 1.07 ± 0.05 μs.

Fig. 4 shows the emission spectrum of $Li_2Sr_{1-x}Ce_xSiO_4$ ($x=0.005$) prepared in a reducing medium of 5% H_2/95% N_2. The emission band extends from 350 to 500 nm and has two maxima at about 397 and 430 nm. Their position is practically independent on the excitation wavelength. It is evident that these maxima are due to transitions from the lowest Ce^{3+} 5d excited state to the 4f ground state levels $^2F_{5/2}$ and $^2F_{7/2}$. The energy gap between the maxima coincides with the spin–orbit splitting of Ce^{3+} ground state, which amounts to about 2000 cm^{-1}. The excitation spectra for $Li_2Sr_{1-x}Ce_xSiO_4$ ($x=0.005$) at 10 K are presented in Fig. 5. The time-integrated excitation spectrum (curves a, b) consists of bands at
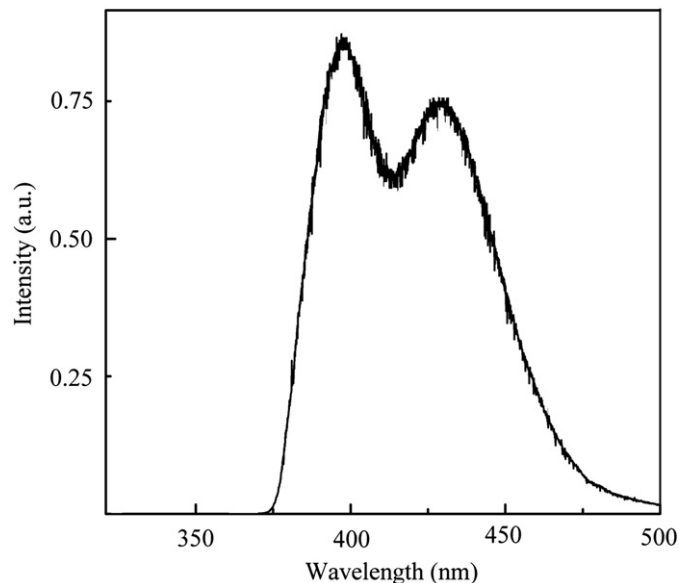

Fig. 4. Emission spectrum of $Li_2Sr_{1-x}Ce_xSiO_4$ ($x=0.005$) prepared in a reducing medium of 5% H_2/95% N_2. The spectrum was recoded at 77 K upon excitation at 360 nm.

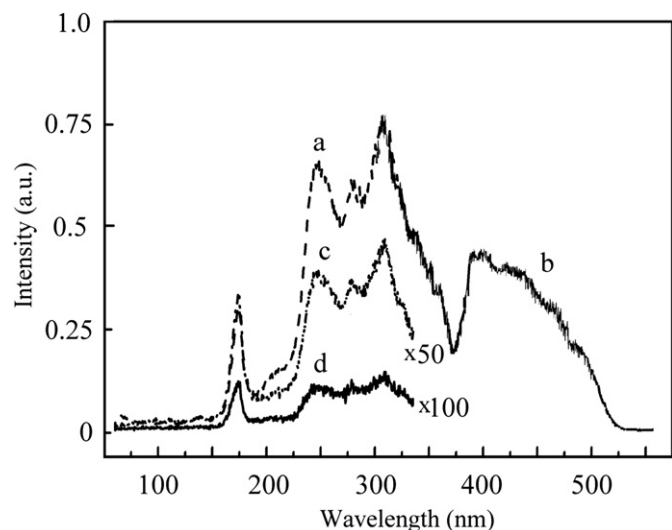**Fig. 3.** Excitation spectra of $Li_2Sr_{1-x}Eu_xSiO_4$ ($x=0.007$) prepared in a reducing medium for the emission at 570 nm at 10 K. The time-integrated spectrum is a superposition of curves (a) and (b) obtained upon excitation with synchrotron radiation and optical photons, respectively. The time-resolved spectra were recorded for two different time intervals after picosecond pulse excitation: (c) between 80 and 180 ns, (d) between 1.5 and 8 ns.

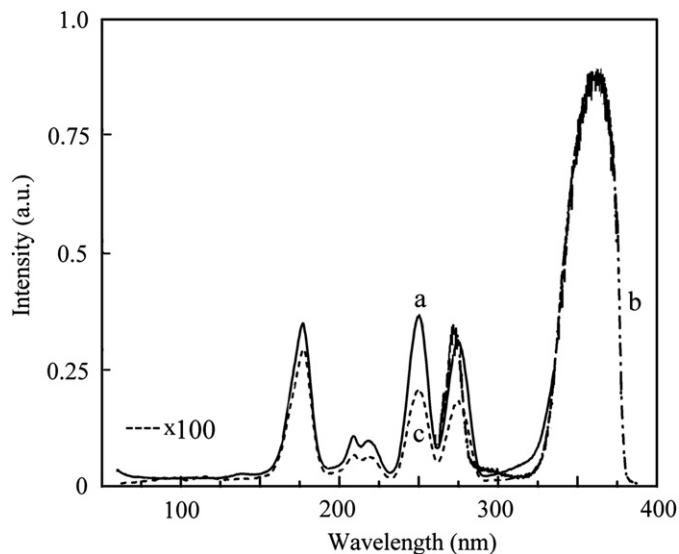**Fig. 5.** Excitation spectra of $Li_2Sr_{1-x}Ce_xSiO_4$ ($x=0.005$) for the emission at 400 nm at 10 K. The time-integrated spectrum is a superposition of curves (a) and (b) obtained upon excitation with synchrotron radiation and optical photons, respectively. The short-time excitation spectrum (curve c) was recorded for time interval between 1.5 and 8 ns after picosecond pulse excitation.

209, 218, 251, 275 and 362 nm. It is evident that these five excitation bands are due to direct excitation of the Ce^{3+} ions via transitions to the components of the $Ce^{3+}5d$ configuration. The lowest excitation band is situated at 362 nm, so that the Stokes shift of the Ce^{3+} emission in Li_2SrSiO_4 is about 2400 cm^{-1}. Since no significant change of the Ce^{3+} emission in $Li_2Sr_{1-x}Ce_xSiO_4$ is observed upon varying the Ce^{3+} concentration in the range $x=0.00001–0.005$, one can conclude that most of the Ce^{3+} ions are present in the form of locally uncompensated $Ce_{Sr}^{.}$ centers. No other Ce^{3+} centers are present in significant amounts. However, for higher x, the formation of Ce^{3+} centers, locally compensated by point defects, can be expected. Recently, Liu at al. [13] have reported the value of 5300 cm^{-1} as the Stokes shift of the emission of $Li_2Sr_{1-x}Ce_xSiO_4$ ($x=0.045$). This differs from that ($\delta=2400$ cm^{-1}) found in the present work. This discrepancy can be explained by the existence of several kinds of cerium centers in the sample studied by Liu et al. [13]. As seen from Fig. 5, in addition to the $4f \rightarrow 5d$ excitation bands, the time-integrated excitation spectrum contains an intense band and with a maximum at about 175 nm (7.08 eV), which was also observed in the excitation spectra for the emission of Eu^{2+}-doped Li_2SrSiO_4. The short-time excitation spectrum (curve c) has the same structure. The $Ce^{3+} 4f \rightarrow 5d$ excitation bands at 209, 218, 251, 278 nm, and the tail of the band at 362 nm are clearly observed. In the 100–180 nm region the spectrum is very similar to those for Li_2SrSiO_4 doped with Eu^{2+} (see Fig. 3).

The decay curves of the Ce^{3+} emission at 10 K for two different excitation wavelengths are presented in Fig. 6. Upon excitation at $\lambda_{exc}=250$ nm the decay is exponential and can be characterized by a time constant (τ) of 39 ± 1 ns. This value is typical for $Ce^{3+} 5d \rightarrow 4f$ transitions. The same result was obtained under excitation of the Ce^{3+} emission in any of the $4f \rightarrow 5d$ bands. Upon excitation at $\lambda_{exc}=175$ nm the decay (Fig. 6, curve b) shows a distinct deviation from the exponential behavior. This confirms that the band at 174 nm (7.12 eV) is caused by host lattice absorption with a subsequent energy transfer to the Ce^{3+} ions. An estimation of the band gap energy (E_g) of Li_2SrSiO_4 can be made taking into account that E_g is roughly $1.08E_{ex}$, where E_{ex} is the energy of the first exciton absorption maximum [17]. From the maximum of the host lattice excitation band at 174 nm (7.12 eV), which was tentatively assigned to the exciton absorption, E_g of Li_2SrSiO_4 was estimated to be 7.69 eV. This value is close to those

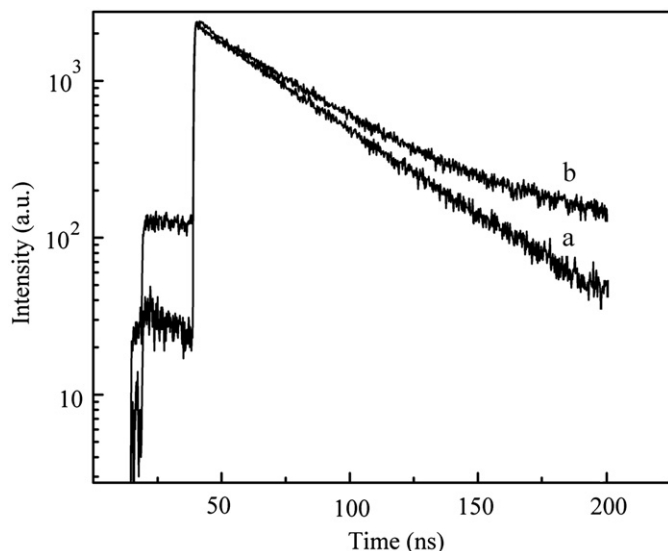**Fig. 6.** Decay curves of the emission at 400 nm of $Li_2Sr_{1-x}Ce_xSiO_4$ ($x=0.005$) recorded upon excitation at 250 nm (a) and 175 nm (b). The measurements were performed at 10 K.

($E_g=7.65–7.85$ eV) reported for $Na(K)AlSi_3O_8$, $CaAl_2Si_2O_8$ [18] and Li_2CaSiO_4 [19].

4. Discussion

The prominent feature of the Eu^{2+}-doped Li_2SrSiO_4 is the spectral position of the emission maximum at very long wavelength. Eu^{2+} luminescence is usually due to $4f^65d \rightarrow 4f^7$ interconfigurational transitions, which lead to a rather broad emission whose spectral position depends strongly on the chemical nature of the crystal. The maximum of the $Eu^{2+} 4f^65d \rightarrow 4f^7$ emission band for alkaline earth silicates and borates typically lies in between 370 and 520 nm; meanwhile, green to yellow and even red emissions have been reported for Eu^{2+} doped Sr_2LiSiO_4F, $BaSiO_3$, $Ba_2LiB_5O_{10}$ and $Ba_2Mg(BO_3)_2$ [20,21]. In all the cases the emission bands are broad and the corresponding Stokes shifts are very large, ranging from ~ 7500 cm^{-1} for $BaSiO_3:Eu^{2+}$, $Sr_2LiSiO_4F:Eu^{2+}$ and up to 12,000 cm^{-1} for $Ba_2Mg(BO_3)_2:Eu^{2+}$. Poort et al. [20,21] and later Dorenbos [22] pointed out that these long-wavelength emissions are possibly not related to the $4f^65d \rightarrow 4f^7$ transitions of Eu^{2+} ions, but may be due to an absolutely different process, namely radiative decay of an impurity trapped exciton. This interpretation implies that excitation into the $Eu^{2+} 4f^7 \rightarrow 4f^65d$ bands leads to ionization of Eu^{2+} ions and the formation of an exciton-like state, which consists of a bound electron hole pair with the hole localized on the Eu^{3+} ion and the electron delocalized on the nearest-neighbor cations. Despite the emission maximum of $Li_2SrSiO_4:Eu^{2+}$ is in between those of $Sr_2LiSiO_4F:Eu^{2+}$ (535 nm), $BaSiO_3:Eu^{2+}$ (550 nm) and $Ba_2LiB_5O_{10}:Eu^{2+}$ (620 nm), this luminescence shows the characteristics of the $Eu^{2+} 4f^65d \rightarrow 4f^7$ ($^8S_{7/2}$) emission. The red shift with the respect to the lowest excitation band is relatively small (3400 cm^{-1}), the decay time ($\tau=1.07$ μs) is typical for $4f^65d \rightarrow 4f^7$ transitions of Eu^{2+} in inorganic compounds [21].

4.1. What factors cause the long-wavelength position of the Eu^{2+} emission in Li_2SrSiO_4?

It is known that the depression in energy position of the lowest $4f^65d$ level of Eu^{2+} ion in a crystal can be considered as a result of two independent contributions, namely the centroid shift E_c, defined as the energy shift of the barycentre of the $Eu^{2+} 4f^65d$ configuration relative to the free ion value ($\sim 34,000$ cm^{-1}), and the total crystal field splitting E_{cfs}, defined as the energy difference between the maxima of the highest and lowest $4f^7 \rightarrow 4f^65d$ bands in the excitation spectra [23,24]. The value of centroid shift E_c mainly depends on the covalency of the Eu^{2+}–ligand bond and the polarizability of the ligands coordinating Eu^{2+}. The crystal field splitting is determined by the size and shape of the coordination polyhedron around Eu^{2+} [23,24].

The complicated energy level scheme of the $Eu^{2+} 4f^65d$ configuration makes difficult the determination of the total crystal splitting and the centroid shift in compounds where, like Li_2SrSiO_4, Eu^{2+} ions occupy sites with low point symmetry. By contrast, the 5d configuration of Ce^{3+} ions in a crystal is typically split into five different crystal-filed components, so that five distinct $4f \rightarrow 5d$ bands are usually observed in excitation and absorption spectra of Ce^{3+} ions. Since the centroid shift, the total crystal splitting of the 5d configuration of Eu^{2+} and Ce^{3+} ions in a crystal are linearly related to one another [23], luminescent characteristics of Ce^{3+} ions in a compound can be used to explain or to predict those of Eu^{2+} in the same compound. The necessary conditions for reasonable conclusions are that in a compound the Ce^{3+} should occupy the same position as Eu^{2+}, and the charge compensating defect should be located outside the first coordination sphere of Ce^{3+}. As

Table 1
Comparison of the luminescent properties of Ce^{3+} ions in some inorganic compounds (N_M is coordination number of Ce^{3+}).

Compound	N_M	E_{cfs} (cm^{-1})	E_c (cm^{-1})	Ref.
Li_2SrSiO_4	8	20,200	11,720	This work
Li_2CaSiO_4	8	19,500	11,580	19
$LiCaPO_4$	8	16,000	9870	19
LaP_3O_9	8	17,100	7990	24
CeP_5O_{14}	8	17,000	7220	24
LaP_5O_{14}	8	16,600	7070	24
$Ca_2Si_5N_8$	6(7)	~13,100	~20,000	27
$Sr_2Si_5N_8$	8(9)	~15,300	~20,500	27

mentioned above (see Section 3), these conditions are realized in the case of $Li_2Sr_{1-x}Ce_xSiO_4$ ($x \leq 0.005$).

In Table 1, the luminescent characteristics of Ce^{3+} ions in Li_2MSiO_4 (M=Ca, Sr) and some other compounds are compared. It is seen that the total crystal field splitting E_{cfs} for Ce^{3+} ions in Li_2SrSiO_4 is quite large for an eightfold coordinated site. The larger E_{cfs} shifts the lowest 5d state to lower energies. Typically, the total crystal field splitting E_{cfs} becomes larger when the radius of the alkaline earth ion decreases. However, the value of E_{cfs} for Ce^{3+} ions in Li_2SrSiO_4 is found to be larger than that of Ce^{3+} ions in Li_2CaSiO_4. This can be assigned to the differences in the coordination polyhedra of the Ce^{3+} ions in these compounds. Also note that the found value of E_{cfs} (20,200 cm^{-1}) essentially differs from that (E_{cfs}=11,400 cm^{-1}) reported for Ce^{3+} ions in Li_2SrSiO_4 by Liu et al. [13]. The most probable explanation is that Liu et al. [13] have used a lamp source with a very low output at wavelengths shorter than 240 nm, so that the excitation bands at 209 and 218 nm were not recorded in their experiments.

The value of E_c (11,720 cm^{-1}) found in the present work for Li_2SrSiO_4:Ce^{3+} is larger than the typical values for phosphates and borates (7000–10,000 cm^{-1}), and is close to, but somewhat smaller than those for chlorides (~13,000 cm^{-1}) [24]. This observation indicates to a relatively large covalency of the metal–oxygen bond in Li_2SrSiO_4. It is interesting to compare the results with the literature data for lanthanide (Ln=Ce^{3+}, Eu^{2+})-doped alkaline-earth silicon nitrides of the composition $M_2Si_5N_8$ (M=Ca, Sr), since these materials were found to have a high potential for white LED's applications [25,26]. It is seen that the values of E_{cfs} for Ce^{3+} in $M_2Si_5N_8$ (13,000–15,000 cm^{-1} [27]) are essentially smaller than that for Li_2SrSiO_4:Ce^{3+}. The very large values of E_c (~20,000 cm^{-1}) indicate that the long-wavelength emissions of Ce^{3+} (and Eu^{2+} too) in $M_2Si_5N_8$ (M=Ca, Sr) [26,27] should be attributed to the high degree of covalency of the Ln–N bond. In contrast to Ln-doped $M_2Si_5N_8$, the influence of the crystal structure of Li_2SrSiO_4 on spectral position of the Eu^{2+} emission maximum is explained as arising from the both contributions, the large crystal field splitting of the 4f^{6}5d configuration and the covalency effect.

4.2. What are the reasons for the low stability of Eu^{2+} ions in Li_2SrSiO_4?

The effect of crystal structure on the stability of chemical elements in a concrete electronic configuration (oxidation state) is of relevance to several areas of materials science, such as superconducting cuprates, colossal magnetoresistive manganese related perovskites and lanthanide (Ln^{2+})-doped phosphors. As mentioned above (see Fig. 1), the stabilization of Eu^{2+} in Li_2SrSiO_4 during the synthesis process requires a strong reducing agent (H_2), even then depending upon the preparation conditions some amount of Eu^{3+} can be revealed in the final products [12]. There are at least two approaches to predict the stability of Ln^{2+} in

inorganic compounds. For simplicity, they will be characterized here as "chemical" and "physical" ones. The "chemical" approach is based on the supposition that the stability of oxidation states of lanthanides in solids is mainly determined by the nature of their coordination polyhedron [28–30]. In this approach, for compounds in which there is no disorder, the valence V_i (the oxidation number) of an atom should be equal to the sum of the individual bond valences (BVS) coordinating the atom [31]:

$$V_i = \sum_j \exp\left[(R_0 - R_{ij})/b\right] \tag{1}$$

where R_{ij} is an observed bond length, R_0 is a tabulated parameter and b is an empirical constant equal to 0.37 Å.

In other words, bonding requirements of oxygen atoms coordinating Eu^{2+} are expected to determine the stability of Eu^{2+} ions in Li_2SrSiO_4. Taking into account that for the Eu(II)–O bond R_0=2.147 Å [31] and using the known values of R_{ij} for Li_2SrSiO_4 [9] and Li_2EuSiO_4 [14], one can obtain a value of 2.17 valence units as the BVS on Eu^{2+} ion. This somewhat exceeds its formal charge, indicating that the Eu^{2+} ions may be relatively unstable in these compounds. The advantage of this approach is that the influence of different point defects on the stability of Ln^{2+} can easily be predicted based on local charge balance considerations. Very recently, Kim et al. [12] have analyzed the chemical composition of Li_2SrSiO_4:Eu (Ce) solid solutions by means of an inductive-coupled plasma atomic-emission spectroscopy and an XANES method. Although the samples under study were prepared in a reducing medium (5% H_2/95% N_2) by solid state reactions between reagents taken in stoichiometric amounts, the results indicated to the presence of Li-vacancies and some amount of Eu^{3+} ions. In terms of this approach, the formation of Li-vacancies should lead to the appearance of underbonded oxygen atoms which, however, can be stabilized by coordination to Eu^{3+} instead of Eu^{2+}. Also, the introduction of Ce^{3+} ions should stabilize the low oxidation state (+2) of europium ions in Li_2SrSiO_4. This prognosis fully agrees with the experimental results by Kim et al. [12].

In the "physical" approach, the stability of Ln^{2+} against oxidation is determined by the location of the Ln^{2+} ground-state level relative to the Fermi level in the undoped compound [32]. One expects that Ln impurity should prefer the oxidation state +2, if the ground-state level of Ln^{2+} is situated just below the Fermi level, and the oxidation state +3, if the ground-state level is situated above the Fermi level. For undoped compounds, the Fermi energy (E_F) is approximately one-half of the band gap energy. Taking into account that the energy of charge transfer from the valence band to an Eu^{3+} (E_{CTS}) determines the location of the ground state of the corresponding Eu^{2+} ion relative to the top of the valence band [32] and using values for E_g (7.65 eV) and E_{CTS} (4.27 eV) found in the present work from the luminescence measurements, one can reveal that the ground-state level of Eu^{2+} in Li_2SrSiO_4 is situated just above the Fermi level (E_F=3.83 eV), i.e. the stability of Eu^{2+} in Li_2SrSiO_4 is expected to be low.

5. Conclusions

The luminescent properties of Eu^{2+} and Ce^{3+} ions in Li_2SrSiO_4 have been studied upon excitation in the 2–20 eV region. The Eu^{2+} ions in Li_2SrSiO_4 exhibit a broad band emission in the 500–750 nm region, which is due to the 4f^{6}5d→4f^7 transition. The red shift of this emission with the respect to the lowest excitation band is relatively small (3400 cm^{-1}), the decay time at 77 K (τ=1.07 μs) is typical for 4f^{6}5d→4f^7 transitions of Eu^{2+} in inorganic compounds. It was shown that the long-wavelength position of the Eu^{2+} emission in Li_2SrSiO_4 (λ_{max}=576 nm) is caused by the large

crystal-field splitting of the Eu^{2+} $4f^65d$ configuration and the relatively high degree of covalency of the Eu–O bond.

The energies of all 5d crystal field levels of Ce^{3+} ions in Li_2SrSiO_4 have been determined. In addition to the $4f \rightarrow 5d$ excitation bands, the excitation spectra of the Ce^{3+} and Eu^{2+} ions emissions show a band with a maximum at 7.12 eV, which is attributed to the host lattice absorption.

The stabilization of Eu^{2+} ions in Li_2SrSiO_4 during the synthesis process requires a strong reducing agent. Two phenomenological approaches to explain the low stability of Eu^{2+} in Li_2SrSiO_4 were discussed. They appear to agree with the experimental observations.

References

[1] A. Mills, III–Vs Rev. 19 (2006) 30.
[2] H. Yamamoto, S. Yasuda, K. Uheda, J. Light Vis. Environ. 32 (2008) 19.
[3] S. Nakamura, G. Fasol, The Blue Laser Diode, Springer, Berlin, 1996.
[4] J.K. Park, C.H. Kim, S.H. Park, H.D. Park, S.Y. Choi, Appl. Phys. Lett. 84 (2004) 1647.
[5] H.S. Jang, D.Y. Jeon, Opt. Lett. 32 (2007) 3444.
[6] K. Toda, Y. Kawakami, S. Kousaka, Y. Ito, A. Komeno, K. Uematsu, M. Sato, IEICE Trans. Electron. E89-C (2006) 1406.
[7] M. Zhang, J. Wang, W. Ding, Q. Zhang, Q. Su, Opt. Mater. 30 (2007) 571.
[8] N. Lakshminarasimhan, U.V. Varadaraju, J. Electrochem. Soc. 152 (2005) H152.
[9] M. Pardha Saradhi, U.V. Varadaraju, Chem. Mater. 18 (2006) 5267.
[10] H. He, R.L. Fu, H. Wang, X. Song, Z. Pan, X. Zhao, X. Zhang, Y. Cao, J. Mater. Res. 23 (2008) 3288.
[11] X. Zhang, H. He, Z. Li, T. Yu, Z. Zou, J. Lumin. 128 (2008) 1876.
[12] T.-G. Kim, H.-S. Lee, C.C. Lin, T. Kim, R.-S. Liu, T.-S. Chan, S.-J. Im, Appl. Phys. Lett. 96 (2010) 061904.
[13] L. Liu, R.-J. Xie, N. Hirosaki, Y. Li, T. Takeda, C.-N. Zhang, J. Li, X. Sun, J. Am. Ceram. Soc. 93 (2010) 2018.
[14] B. Haferkorn, G. Meyer, Z. Anorg, Allg. Chem. 624 (1998) 1079.
[15] G. Zimmerer, Radiat. Meas. 42 (2007) 859.
[16] Z. Qi, C. Shi, M. Liu, D. Zhou, X. Luo, J. Zhang, Y. Xie, Phys. Status Solidi A 201 (2004) 3109.
[17] P. Dorenbos, J. Lumin. 111 (2005) 89.
[18] A.E.R. Malins, N.R.J. Poolton, F.M. Quinn, O. Johnsen, P.M. Denby, J. Phys. D: Appl. Phys. 37 (2004) 1439.
[19] P. Dorenbos, L. Pierron, L. Dinca, C.W.E. van Eijk, A. Kahn-Harari, B. Viana, J. Phys. Condens. Matter. 15 (2003) 511.
[20] S.H.M. Poort, H.M. Reijnhoudt, H.O.T. van der Kuip, G. Blasse, J. Alloys Compd. 241 (1996) 75.
[21] S.H.M. Poort, A. Meyerink, G. Blasse, J. Phys. Chem. Solids 58 (1997) 1451.
[22] P. Dorenbos, J. Lumin. 104 (2003) 239.
[23] P. Dorenbos, Phys. Rev. B 64 (2001) 125117.
[24] P. Dorenbos, J. Phys.: Condens. Matter 15 (2003) 4797.
[25] R. Mueller-Mach, G. Mueller, M.R. Krames, H. Hoppe, F. Stadler, W. Schnick, T. Juestel, P. Schmidt, Phys. Status Solidi A 202 (2005) 1727.
[26] Y.Q. Li, J.E.J. van Steen, J.W.H. van Krevel, G. Botty, A.C.A. Delsing, F.J. DiSalvo, G. de With, H.T. Hintzen, J. Alloys Compd. 417 (2006) 273.
[27] Y.Q. Li, G. de With, H.T. Hitzen, J. Lumin. 116 (2006) 107.
[28] Yu.M. Kiselev, Russ. J. Inorg. Chem. 43 (1998) 688.
[29] V.P. Dotsenko, I.V. Berezovskaya, N.P. Efryushina, A.S. Voloshinovskii, G.B. Stryganyuk, Radiat. Meas. 42 (2007) 803.
[30] V.P. Dotsenko, I.V. Berezovskaya, N.P. Efryushina, Handbook on Borates: Chemistry, Production and Applications, in: M.P. Chung (Ed.), Nova Science Publishers, Inc., New York2009, pp. 59–105.
[31] N.E. Brese, M. OKeeffe, Acta Crystallogr. B 47 (1991) 192.
[32] P. Dorenbos, Chem. Mater. 17 (2005) 6452.